NeuroImage: Clinical 31 (2021) 102770

Contents lists available at ScienceDirect

NeuroImage: Clinical

journal homepage: www.elsevier.com/locate/ynicl

Altered microstructural pattern of white matter in Cushing's disease identified by automated fiber quantification

Mengchu Cui [a,b], Tao Zhou [b], Shiyu Feng [b], Xinyun Liu [c], Fuyu Wang [b], Yanyang Zhang [b,*], Xinguang Yu [b,*]

[a] Medical School of Chinese PLA, Beijing, PR China
[b] Department of Neurosurgery, The First Medical Centre, Chinese PLA General Hospital, Beijing, PR China
[c] Department of Radiology, The First Medical Centre, Chinese PLA General Hospital, Beijing, PR China

ARTICLE INFO

Keywords:
Cushing's disease
White mater
Hypercortisolism
Diffusion tensor imaging
Automated fiber quantification

ABSTRACT

A growing body of evidence suggests that altered brain structure plays a crucial role in the pathogenesis of neuropsychological abnormalities induced by hypercortisolism in patients with Cushing's disease. While most studies mainly focus on gray matter, white matter structure has been largely overlooked. In the current study, we conducted a cross-sectional diffusion tensor imaging study on 58 patients with Cushing's disease and 54 matched healthy individuals to profile the microstructural pattern using automated fiber quantification and investigate its association with neuroendocrine and neuropsychological deficits. The study revealed that microstructural pattern showed a widespread mean diffusivity, radial diffusivity increase, fractional anisotropy decrease and partial axial diffusivity increase among tracts notably in corpus callosum forceps, inferior fronto-occipital fasciculus, inferior longitudinal fasciculus, superior longitudinal fasciculus, uncinate fasciculus and arcuate fasciculus, while within the same tract abnormalities localized to specific positions. Moreover, compromised microstructural pattern of white matter in specific tracts and locations along the trajectory were associated with ACTH and cortisol concentration and cognitive decline in patients with Cushing's disease. Collectively, our study elucidates the form of white matter pathology induced by hypercortisolism and its association with cognitive decline which may provide further targets for early identification and intervention of Cushing's disease.

1. Introduction

Cushing's disease is characterized by excess endogenous cortisol production resulting from the presence of an adrenocorticotropic hormone (ACTH)-producing pituitary adenoma (Lacroix et al., 2015) and represent a natural human model for investigating the chronic effects of excess endogenous cortisol on brain physiology (van der Werff et al., 2015). In addition to physical symptoms, prolonged exposure to excess cortisol would also cause a variety of deleterious effects on the vulnerable brain which is abundant with cortisol receptor (Alonso, 2000), resulting in grievous neurocognitive impairments and neuropsychological symptoms (Forget et al., 2000; León-Carrión et al., 2009; Piasecka et al., 2020; Sonino and Fava, 2001) including memory loss, lack of concentration, impaired executive function, depression, apathy, psychosis and anxiety (Lacroix et al., 2015; Piasecka et al., 2020). Since neuropsychological disorders have long been thought to involve ineffective and insufficient orchestration between different brain areas (Friston, 1998), some of the researchers tried to identify the relationship between brain structure and hypercortisolism according to these affective and cognitive deficits exhibited in Cushing's disease (Jiang et al., 2017a; Pires et al., 2015; Pires et al., 2017).

Based on autopsy, Trethowan and Cobb found brain weight loss and enlarged ventricles in patients with Cushing's disease for the first time (Trethowan and Cobb, 1952). Findings were later supported by an in vivo study which showed a high incidence of atrophy in the whole brain using pneumoencephalography (Momose et al., 1971). With the introduction of neuroimaging, voxel-based morphometry was applied to investigate brain structure mainly on gray matter (van der Werff et al., 2014) and specific regions were reported successively. For instance, Starkman et al. reported smaller hippocampus which was related to memory loss induced by hypercortisolism in patients with Cushing's syndrome (Starkman et al., 1992). Andela et al. showed a reduction in

* Corresponding authors at: Department of Neurosurgery, The First Medical Centre, Chinese PLA General Hospital, 28 Fuxing Road, Haidian District, Beijing 100853, PR China.
E-mail addresses: sjwkzyy@163.com (Y. Zhang), xinguang_yu@263.net (X. Yu).

https://doi.org/10.1016/j.nicl.2021.102770
Received 22 April 2021; Received in revised form 26 June 2021; Accepted 20 July 2021
Available online 24 July 2021

the volume of anterior cingulate cortex as well as cortical thickness (Andela et al., 2013). Jiang et al revealed decreased volumes in the medial frontal gyrus (Jiang et al., 2017b) and smaller amygdala were reported by by santos and his colleagues (Santos et al., 2017). However, most of the neuropsychological deficits persist even after resolution of hypercortisolism when the volume of gray matter partially restored while alterations of white matter tend to be independent of concomitant hypercortisolism (Jiang et al., 2019; Pires et al., 2017).

White matter comprises intensively bundled, mostly myelinated axons that interconnect gray matter regions, microstructural pattern of white matter has been considered a critical factor in the pathogenesis of mental disorder (Friston, 1998). Using diffusion tensor imaging, neuroimaging researches targeting regions of interest (ROIs) and using voxel-wise statistical analysis and tract-based spatial statistics (TBSS) have reported widespread reductions of white matter integrity in patients with Cushing's disease (Pires et al., 2017; van der Werff et al., 2014). However the alterations of white matter were investigated only in an explorative way for the related studies were very limited and detailed locations and range of tracts remained elucidated (Bauduin et al., 2018). Collectively, the understanding of microstructural pattern of white matter in patients with Cushing's disease may provide a deeper insight into the pathogenesis of hypercortisolism-induced neuropsychological disorders and new targets for early identification and intervention of Cushing's disease.

To address these issues, we acquired structural magnetic resonance image and diffusion tensor image from 58 patients with Cushing's disease and 54 sex-, age- and education- matched healthy individuals to characterize diffusion properties of major fiber tracts. Since different clusters of axons exit and enter the tract and disease strikes at specific locations within the tract, the tissue properties would vary along each fiber tract (Hattori et al., 2011). Hence, we performed automated fiber quantification (AFQ), a new algorithm that could automate identified 20 main fiber tracts including association tracts, projection tracts and commissural tracts, and profile diffusion properties at anatomically equivalent locations along the trajectories (Yeatman et al., 2012) to investigate microstructural pattern of white matter in patients with Cushing's disease. Dose effect on diffusion properties and relationship of diffusion metrics with psychological and cognitive performance were studied in general and particular ways as well.

2. Materials & Methods

2.1. Subjects

In this study implemented from May 2017 to November 2020, 114 right-handed subjects with normal vision and auditory sensation were recruited by The First Medical Center of Chinese People's Liberation Army General Hospital, including 60 CD patients (4 males and 56 females; mean age 37.8; age range 15–62) and 54 matched healthy control individuals (3 males and 51 females; mean age 34.6; age range 19–63) in terms of sex, age and education. All participants were carefully interviewed to ensure the absence of present or past mental disorder and history of psychiatric drug exposure. Other brain structural abnormalities (e.g., tumor, trauma, cerebrovascular disease) were ruled out by brain imaging. 2 CD patients were excluded before image analysis because of poor DTI image quality (see Supplementary material for a detailed description of quality control).

Diagnosis of CD patients was determined by experienced endocrinologists and neurosurgeons according to latest clinical guideline after excluding exogenous cortisol exposure (Nieman et al., 2015): functional diagnosis to confirm the presence of endogenous hypercortisolism: clinical features related to excess cortisol exposure (e.g. central obesity, moon face, dorsocervical fat pad, purpura, diabetes, hypertension, immunosuppression, psychiatric deficits and neurocognitive deficits), elevated cortisol secretion rates (reference range at 8 am: 198.7–797.5 nmol/L), 24-hour urinary free cortisol (24 h-UFC, reference range 98.0–500.1 nmol/24 h), late-night salivary cortisol (>4 nmol/L), absence of low-dose dexamethasone suppression (1 mg overnight or 2 mg/d for 48 h) and abnormal cortisol circadian; Etiologic diagnosis to identify ACTH dependent or independent: normal or high serum ACTH (reference range at 8 am: <10.12 pmol/L); localization diagnosis to determine eutopic or ectopic: existence of high-dose dexamethasone suppression (>50% suppressed, 8 mg/d for 48 h) and positive dynamic gadolinium-enhanced pituitary MRI. Inferior petrosal sinus sampling was used when results were discordant and CD diagnosis was confirmed by postsurgical pathology.

This study was approved by the ethics committee of the Chinese PLA General Hospital, Beijing, China; written informed consent was obtained from each participant. The data has been used in our previous studies (Wang et al., 2019; Zhang et al., 2021).

2.2. Neuroendocrine and neuropsychological assessment

Biochemical assessments including 24 h-UFC, serum cortisol (nmol/L) and plasma ACTH (pmol/L) at 0:00, 8:00 and 16:00 were performed to quantify the functional status of HPA in CD patients. Cortisol and ACTH of 8:00, 24 h-UFC were measured in healthy control individuals as comparisons. All the assays were completed in a standardized examination workflow before surgery.

All participants received Mini-mental State Examination (MMSE, scores range from 0 to 30, a lower score means more severe mental impairment), Montreal Cognitive Assessment (MoCA, scores range from 0 to 30, a lower score means greater cognitive impairment), Self-Rating Depression Scale (SDS, scores < 53: "normal", 53–62: "mild depression", 63–72 "moderate depression", >73 "severe depression") and Self-Rating Anxiety Scale (SAS, scores <50: "normal",50–59: "mild anxiety",60–69 "moderate anxiety", >69 "severe anxiety") to reflect the mental status. Moreover, Cushing's Quality of Life questionnaire and Chinese version of neuropsychiatric inventory (scores range from 0 to 144, a higher score indicating worse psychiatric status) were used to evaluate disease-related life quality and neuropsychiatric symptoms of CD patients. All the assessments were implemented preoperatively by an experienced practitioner who was blinded to the grouping.

2.3. Magnetic resonance imaging acquisition

A set of 3.0 T Magnetic resonance imaging system with an eight-channel phase array head coil (Discovery MR750, General Electric) was introduced to acquire images from subjects. Diffusion weighted images including both 64 diffusion-encoding directions (b = 1000 s/mm^2) and no diffusion encoding (b = 0 s/mm^2) were collected using a spin-echo planar imaging sequence (EPI) with the following parameters: TR: 6943 ms, TE: 80.8 ms, FOV: 224 × 224 mm, number of slices: 65, slice thickness: 2 mm with no gap. High-resolution 3-dimensional T1 weighted structural images were acquired for registration using a sagittal fast spoiled gradient-echo sequence with parameters of TR: 6.7 ms, TE: 2.9 ms, flip angel: 7°, FOV: 256 × 256 mm^2, number of slices: 192, slice thickness: 1 mm with no gap. Scans were conducted and reviewed by experienced neuroradiologists. Signal-to-noise ratio (SNR), artifacts and head motion of MR images were examined for quality control as well.

2.4. Magnetic resonance image preprocessing

FSL software (FMIRB Software Library, Oxford Center for Functional MRI of the Brain, University of Oxford, UK) (Jenkinson et al., 2012) was introduced to perform preprocessing of raw MRI data. To correct image distortion induced by slight head motion and eddy current, FLIRT (FMRIB's Linear Image Registration Tool) (Jenkinson and Smith, 2001) was applied to affinely coregister all diffusion-weighted images to the b0 image with 12 degrees of freedom. Transformation matrices were extracted to rotate the diffusion gradient directions. BET (Brain

Extraction Tool) (Smith, 2002) was used to acquire brain masks (to remove non-brain tissues) of T1 and b0 images with a fractional intensity threshold at 0.2. The diffusion tensor model was fitted using FDT (FMRIB's Diffusion Tool) with corrected diffusion gradient direction matrices to reconstruct diffusion tensor, fractional anisotropy (FA), mean diffusivity (MD), axial diffusivity (AD) and radial diffusivity (RD) images were produced at the same time.

2.5. Automated fiber quantification

Automated fiber quantification (AFQ) (Yeatman et al., 2012) software is an open-source MATLAB-based software package, which can automatedly identify 20 main tracts (cingulum was divided into cingulum cingulate and cingulum hippocampus, arcuate fasciculus was separated from the superior longitudinal fasciculus) and map the diffusion tensor to the finely segmented tract profile according to the identification method raised by Hua et al. (2008) and Zhang et al. (2008). Procedures of AFQ could be summarized as follows: Firstly, whole-brain tractography: a streamlines tracking algorithm with a fourth-order Runge-Kutta path integration method was introduced to trace whole-brain fibers within the brain mask (Basser et al., 2000); Secondly, fiber tract segmentation and refinement, each fiber tract was isolated from the whole brain fiber group using waypoint ROIs (predefined ROIs) approach developed by Wakana et al. (2007) and refined by comparing candidate fiber tract with fiber tract probability map (JHU white-matter tractography atlas) introduced by Hua et al. (2008). Thirdly, fiber tract cleaning, an iterative procedure was implemented to remove the outliers which deviated (>5 standard deviations) from the core of the tract or were longer (>4 standard deviations) than the mean fiber length according to a Gaussian distribution; Fourthly, fiber tract clipping, each fiber tract was clipped into central portion spanning between the two waypoints ROIs for its consistency in different individuals; finally, fiber tract quantification, diffusion tensor was calculated along the trajectory of the central portion of each fiber tract. Thereby, we acquired detailed profiles (100 nodes of the tracts) of 20 main tracts. List of 20 primary tracts: bilateral anterior thalamus radiation (ATR), corticospinal tract (CST), cingulum cingulate (CGC), cingulum hippocampus (CGH), inferior fronto-occipital fasciculus (IFOF), inferior longitudinal fasciculus (ILF), superior longitudinal fasciculus (SLF), uncinated fasciculus (UF), arcuate fasciculus (AF), callosum forceps major (posterior forceps of corpus callosum, CCF_P) and minor (anterior forceps of corpus callosum, CCF_A).

2.6. Statistical analysis

Continuous variables of demographic and clinical indicators were compared between CD patients and healthy control individuals using two-sample T-tests. Categorical variables were compared using Pearson Chi-square test. Mean diffusion properties of 20 tracts were compared using a two-sample T-test with the false discovery rate (FDR, $q < 0.05$) implemented to perform multiple comparison correction with age, sex and education as covariates. SPSS version 22.0 (SPSS) was introduced to perform these analyses. For the pointwise comparison, considering the comparison of each node along the tract profile should not be considered independent and the distributions of the profiles were unknown given the high degree of auto correlation and spatial correlation between different nodes along the tracts. (Yeatman et al., 2012), we organized the tract profile of subjects into matrices and fed them into nonparametric permutation-based statistical analysis for 10,000 permutations with age, sex and education as covariates using the FSL "randomize" command. The statistical results were subsequently subject to family-wise error correction for multiple comparisons following threshold-free cluster enhancement with a threshold of $p < 0.05$ (Sun et al., 2015). To reveal the relationship between clinical symptoms and diffusion properties (FA and MD) of fiber tracts, correlation analysis between clinical indicators and diffusion properties (FA and MD) of significantly changed tracts and locations along the fiber relative to HC individuals were performed by SPSS within the CD patient group using partial Pearson correlation while controlling for age, sex and education.

3. Results

3.1. Group differences in demographics and clinical characteristics

58 CD patients and 54 healthy control individuals were finally included in our cohort. Demographics and clinical characteristics of CD patients and healthy control individuals are presented in Table 1. There were no significant differences ($p > 0.05$) between the two groups in sex composition, age and education. For neurocognitive and neuropsychological assessment, CD patients exhibited significant cognitive impairment, anxiety and depression based on the lower score of MMSE and MoCA and higher scores of SDS and SAS compared with the HC group. Moreover, elevated CNPI and Cushing QOL scores indicated disease-related mental impairment and disturbance of life quality in CD patients. For biochemical indicators, CD patients showed elevated level of serum cortisol, plasma ACTH and 24-h UFC and disturbance of normal cortisol circadian rhythm corresponding with the endocrinological features of Cushing's syndrome. Serum cortisol and plasma ACTH at 8:00 of CD patients were significantly higher compared with the HC group.

Table 1
Demographics and clinical characteristics of participants.

	CD patients (n = 58)	Health control (n = 54)	t / X^2	P-value
Sex (male/female)	5 / 53	3 / 51	0.396	0.529
Age (years)	37.86 ± 10.68	34.59 ± 10.72	1.616	0.109
Education (years)	11.24 ± 4.20	11.80 ± 3.10	−0.800	0.426
Duration of illness (months)	44.87 ± 52.57	N.A.	N.A.	N.A.
Neuropsychological tests				
MMSE	27.94 ± 2.40 (n = 51)	29.28 ± 0.93 (n = 53)	−3.729	<0.001
MoCA	22.45 ± 4.22 (n = 51)	27.70 ± 2.00 (n = 53)	−8.062	<0.001
SDS	40.17 ± 9.72 (n = 52)	27.06 ± 4.42 (n = 53)	8.872	<0.001
SAS	37.71 ± 8.04 (n = 52)	26.96 ± 4.46 (n = 53)	8.448	<0.001
CNPI	12.20 ± 10.23 (n = 54)	N.A.	N.A.	N.A.
Cushing QOL	36.62 ± 8.50 (n = 52)	N.A.	N.A.	N.A.
Serum cortisol (nmol/L)				
0 am	610.32 ± 234.69 (n = 55)	N.A.	N.A.	N.A.
8 am	728.51 ± 279.93	359.82 ± 106.79 (n = 52)	9.304	<0.001
4 pm	651.44 ± 265.85 (n = 57)	N.A.	N.A.	N.A.
ACTH (pmol/L)				
0 am	15.80 ± 10.25 (n = 54)	N.A.	N.A.	N.A.
8 am	20.90 ± 16.22	5.00 ± 3.09 (n = 52)	7.318	<0.001
4 pm	19.94 ± 13.87 (n = 57)	N.A.	N.A.	N.A.
24 h-UFC (nmol/24 h)	2349.09 ± 1554.24 (n = 49)	252.29 ± 119.68 (n = 47)	9.414	<0.001

Data are presented as means ± standard deviations.
Abbreviation: N.A., not applicable; CD, Cushing's disease; MMSE, Mini-Mental State Examination; MoCA, Montreal Cognitive Assessment; SDS, Self-Rating Depression Scale; SAS, Self-Rating Anxiety Scale; CNPI, Chinese version of the neuropsychiatric inventory; Cushing QOL, Cushing's Quality of Life questionnaire; ACTH, adrenocorticotropic hormone; 24 h-UFC, 24 h-urinary free cortisol.

3.2. Group differences in mean diffusion properties

Fiber tracts with 2 waypoint ROIs were reconstructed in 3-dimensional way using the AFQ software package (presented in Supplementary Fig. 2). With regards to diffusion properties, we first inspected them in an overall manner. Group differences in mean diffusion properties were presented in Table 2–5. Since AFQ was an automated algorithm with threshold setting, different anatomical features (distance to gray matter) and diffusion properties of tracts may result in failed fiber tracking, especially bilateral cingulum hippocampus and right arcuate fasciculus. For each fiber, the number of successfully tracked subjects in two groups was listed in column P:N. For the group comparison of mean FA, CD patients showed significant FA reduction relative to HC individuals in CCF, left IFOF, left UF, bilateral ILF, SLF and AF (Table 2, $p < 0.05$, FDR corrected); For the group comparison of mean MD, CD patients showed significant MD elevation relative to HC individuals in the majority of 20 fiber tracts except for right ATR and bilateral CGH (Table 3, $p < 0.05$, FDR corrected); For the group comparison of mean AD, CD patients showed significant AD elevation relative to HC individuals in right CGC, bilateral CST, IFOF, ILF, SLF, UF and AF (Table 4, $p < 0.05$, FDR corrected); For the group comparison of mean RD, CD patients showed significant RD elevation relative to HC individuals in the majority of 20 fiber tracts except for right ATR, bilateral CST and CGH (Table 5, $p < 0.05$, FDR corrected).

3.3. Group differences in tract profile of diffusion properties

Different from traditional tractography, diffusion measurements along the trajectory of white matter fiber tracts could be quantified by the AFQ software to show detailed diffusion properties of tracts. Pointwise comparisons of diffusion properties between CD patients and HC individuals were illustrated in Fig. 1 (FA and MD) and Fig. 2 (AD and RD).

For pointwise comparison of FA profiles, CD patients showed extensive FA reduction in the following certain locations of the tracts: the occipital lobe portion of posterior CCF, the left portion of anterior CCF, the posterior portion of left IFOF, the posterior and intermediate portion of left ILF, the anterior and posterior portion of right ILF, the posterior portion of right SLF, the frontal lobe portion of left UF, the temporal lobe portion of left AF, and the intermediate portion of right AF, as well as some regional segments in the right and intermediate portion of anterior CCF, the anterior and posterior portion of right IFOF,

Table 2
Comparison of mean FA between groups.

Tract	P:N	CD patients (n = 58)	Healthy control (n = 54)	t-value	p-value
ATR_L	58:54	0.427 ± 0.037	0.434 ± 0.021	−1.169	0.321
ATR_R	57:54	0.436 ± 0.037	0.436 ± 0.024	−0.011	0.991
CST_L	58:54	0.620 ± 0.028	0.612 ± 0.023	1.626	0.153
CST_R	58:54	0.603 ± 0.025	0.600 ± 0.021	0.420	0.711
CGC_L	58:54	0.462 ± 0.038	0.479 ± 0.044	−2.144	0.062
CGC_R	58:54	0.436 ± 0.038	0.443 ± 0.042	−1.042	0.353
CGH_L	54:51	0.380 ± 0.042	0.370 ± 0.047	1.141	0.321
CGH_R	56:49	0.375 ± 0.037	0.381 ± 0.039	−0.700	0.540
CCF_P	58:54	0.579 ± 0.067	0.621 ± 0.035	−4.051	<0.001
CCF_A	58:54	0.519 ± 0.039	0.548 ± 0.022	−4.933	<0.001
IFOF_L	58:54	0.430 ± 0.039	0.456 ± 0.029	−4.111	<0.001
IFOF_R	57:54	0.441 ± 0.031	0.452 ± 0.027	−1.975	0.078
ILF_L	58:54	0.401 ± 0.041	0.433 ± 0.030	−4.650	<0.001
ILF_R	58:54	0.389 ± 0.040	0.413 ± 0.029	−3.661	0.001
SLF_L	58:54	0.396 ± 0.036	0.414 ± 0.037	−2.680	0.017
SLF_R	58:54	0.439 ± 0.036	0.464 ± 0.039	−3.573	0.001
UF_L	58:54	0.411 ± 0.035	0.432 ± 0.028	−3.526	0.002
UF_R	58:54	0.396 ± 0.027	0.406 ± 0.025	−2.006	0.078
AF_L	58:54	0.451 ± 0.034	0.478 ± 0.026	−4.602	<0.001
AF_R	48:50	0.419 ± 0.037	0.449 ± 0.036	−3.973	<0.001

Data are presented as means ± standard deviations.
Abbreviation: CD, Cushing's disease; ATR, anterior thalamic radiation; CST, corticospinal tract; CGC, cingulum cingulate; CGH, cingulum hippocampus; CCF, corpus callosum forceps; IFOF, inferior fronto-occipital fasciculus; ILF, inferior longitudinal fasciculus; SLF, superior longitudinal fasciculus; UF, uncinated fasciculus. AF, arcuate fasciculus. L, left; R, right; P, posterior; A, anterior; P: N means the successfully traced number of Cushing's disease patients and healthy control subjects in each fiber.

Table 3
Comparison of mean MD between groups.

Tract	P:N	CD patients (n = 58)	Healthy control (n = 54)	t-value	p-value
ATR_L	58:54	0.782 ± 0.049	0.764 ± 0.021	2.499	0.018
ATR_R	57:54	0.790 ± 0.041	0.778 ± 0.018	1.945	0.061
CST_L	58:54	0.765 ± 0.029	0.751 ± 0.012	3.458	0.001
CST_R	58:54	0.772 ± 0.029	0.761 ± 0.013	2.826	0.008
CGC_L	58:54	0.793 ± 0.034	0.775 ± 0.022	3.358	0.001
CGC_R	58:54	0.797 ± 0.037	0.774 ± 0.023	3.903	<0.001
CGH_L	54:51	0.803 ± 0.039	0.815 ± 0.034	−1.766	0.084
CGH_R	56:49	0.792 ± 0.045	0.801 ± 0.034	−1.204	0.232
CCF_P	58:54	0.894 ± 0.070	0.857 ± 0.051	3.182	0.003
CCF_A	58:54	0.849 ± 0.048	0.821 ± 0.026	3.853	<0.001
IFOF_L	58:54	0.849 ± 0.050	0.806 ± 0.023	5.864	<0.001
IFOF_R	57:54	0.846 ± 0.046	0.815 ± 0.021	4.613	<0.001
ILF_L	58:54	0.852 ± 0.049	0.808 ± 0.027	6.114	<0.001
ILF_R	58:54	0.853 ± 0.051	0.817 ± 0.022	5.025	<0.001
SLF_L	58:54	0.773 ± 0.041	0.734 ± 0.019	6.329	<0.001
SLF_R	58:54	0.765 ± 0.045	0.730 ± 0.018	5.418	<0.001
UF_L	58:54	0.810 ± 0.042	0.7779 ± 0.025	4.662	<0.001
UF_R	58:54	0.853 ± 0.038	0.831 ± 0.027	3.589	<0.001
AF_L	58:54	0.783 ± 0.047	0.740 ± 0.018	6.388	<0.001
AF_R	48:50	0.770 ± 0.046	0.732 ± 0.022	5.143	<0.001

Data are presented as means ± standard deviations.
Abbreviation: CD, Cushing's disease; ATR, anterior thalamic radiation; CST, corticospinal tract; CGC, cingulum cingulate; CGH, cingulum hippocampus; CCF, corpus callosum forceps; IFOF, inferior fronto-occipital fasciculus; ILF, inferior longitudinal fasciculus; SLF, superior longitudinal fasciculus; UF, uncinated fasciculus. AF, arcuate fasciculus. L, left; R, right; P, posterior; A, anterior; P: N means the successfully traced number of Cushing's disease patients and healthy control subjects in each fiber.

Table 4
Comparison of mean AD between groups.

Tract	P:N	CD patients (n = 58)	Healthy control (n = 54)	t-value	p-value
ATR_L	58:54	1.177 ± 0.055	1.161 ± 0.032	1.846	0.093
ATR_R	57:54	1.202 ± 0.053	1.188 ± 0.033	1.763	0.101
CST_L	58:54	1.394 ± 0.046	1.360 ± 0.036	4.365	<0.001
CST_R	58:54	1.384 ± 0.045	1.364 ± 0.032	2.845	0.018
CGC_L	58:54	1.240 ± 0.062	1.232 ± 0.044	0.765	0.495
CGC_R	58:54	1.212 ± 0.061	1.188 ± 0.045	2.410	0.029
CGH_L	54:51	1.164 ± 0.058	1.172 ± 0.045	−0.815	0.491
CGH_R	56:49	1.140 ± 0.063	1.161 ± 0.048	−1.833	0.093
CCF_P	58:54	1.580 ± 0.112	1.578 ± 0.058	0.135	0.925
CCF_A	58:54	1.419 ± 0.048	1.418 ± 0.043	0.094	0.925
IFOF_L	58:54	1.280 ± 0.058	1.248 ± 0.040	3.350	0.004
IFOF_R	57:54	1.287 ± 0.058	1.254 ± 0.036	3.641	0.002
ILF_L	58:54	1.251 ± 0.062	1.221 ± 0.049	2.787	0.018
ILF_R	58:54	1.231 ± 0.064	1.204 ± 0.042	2.658	0.023
SLF_L	58:54	1.115 ± 0.052	1.081 ± 0.044	3.657	0.002
SLF_R	58:54	1.154 ± 0.066	1.127 ± 0.046	2.488	0.026
UF_L	58:54	1.202 ± 0.043	1.183 ± 0.037	2.587	0.024
UF_R	58:54	1.248 ± 0.046	1.228 ± 0.042	2.346	0.032
AF_L	58:54	1.191 ± 0.060	1.152 ± 0.043	3.996	0.001
AF_R	48:50	1.146 ± 0.063	1.120 ± 0.036	2.569	0.024

Data are presented as means ± standard deviations.
Abbreviation: CD, Cushing's disease; ATR, anterior thalamic radiation; CST, corticospinal tract; CGC, cingulum cingulate; CGH, cingulum hippocampus; CCF, corpus callosum forceps; IFOF, inferior fronto-occipital fasciculus; ILF, inferior longitudinal fasciculus; SLF, superior longitudinal fasciculus; UF, uncinated fasciculus. AF, arcuate fasciculus. L, left; R, right; P, posterior; A, anterior; P: N means the successfully traced number of Cushing's disease patients and healthy control subjects in each fiber.

Table 5
Comparison of mean RD between groups.

Tract	P:N	CD patients (n = 58)	Healthy control (n = 54)	t-value	p-value
ATR_L	58:54	0.585 ± 0.054	0.566 ± 0.023	2.398	0.025
ATR_R	57:54	0.583 ± 0.047	0.573 ± 0.022	1.494	0.155
CST_L	58:54	0.451 ± 0.033	0.447 ± 0.018	0.883	0.400
CST_R	58:54	0.467 ± 0.031	0.459 ± 0.017	1.559	0.144
CGC_L	58:54	0.569 ± 0.038	0.546 ± 0.038	3.207	0.003
CGC_R	58:54	0.589 ± 0.041	0.567 ± 0.036	3.003	0.005
CGH_L	54:51	0.622 ± 0.045	0.637 ± 0.048	−1.658	0.125
CGH_R	56:49	0.617 ± 0.048	0.621 ± 0.041	−0.463	0.644
CCF_P	58:54	0.550 ± 0.079	0.496 ± 0.057	4.161	<0.001
CCF_A	58:54	0.564 ± 0.058	0.522 ± 0.027	4.867	<0.001
IFOF_L	58:54	0.633 ± 0.057	0.584 ± 0.029	5.716	<0.001
IFOF_R	57:54	0.625 ± 0.048	0.594 ± 0.026	4.148	<0.001
ILF_L	58:54	0.653 ± 0.055	0.601 ± 0.030	6.309	<0.001
ILF_R	58:54	0.665 ± 0.056	0.623 ± 0.027	5.086	<0.001
SLF_L	58:54	0.601 ± 0.045	0.561 ± 0.025	5.902	<0.001
SLF_R	58:54	0.570 ± 0.046	0.531 ± 0.031	5.209	<0.001
UF_L	58:54	0.613 ± 0.049	0.578 ± 0.031	4.647	<0.001
UF_R	58:54	0.656 ± 0.040	0.632 ± 0.029	3.603	<0.001
AF_L	58:54	0.578 ± 0.050	0.534 ± 0.023	6.086	<0.001
AF_R	48:50	0.582 ± 0.048	0.539 ± 0.033	5.163	<0.001

Data are presented as means ± standard deviations;
Abbreviation: CD, Cushing's disease; ATR, anterior thalamic radiation; CST, corticospinal tract; CGC, cingulum cingulate; CGH, cingulum hippocampus; CCF, corpus callosum forceps; IFOF, inferior fronto-occipital fasciculus; ILF, inferior longitudinal fasciculus; SLF, superior longitudinal fasciculus; UF, uncinated fasciculus. AF, arcuate fasciculus. L, left; R, right; P, posterior; A, anterior; P: N means the successfully traced number of Cushing's disease patients and healthy control subjects in each fiber.

the anterior portion of the left ILF and the temporal lobe portion of right AF.

For pointwise comparison of MD, CD patients showed widespread MD elevation in the following certain locations of the tracts: the anterior portion of left ATR, the anterior and intermediate portion of right ATR, the superior and inferior portion of bilateral CST, the posterior portion of right CGC, the occipital lobe portion of posterior CCF, the frontal lobe portion of anterior CCF, the anterior and posterior portion of bilateral IFOF, the entire bilateral ILF and SLF, the temporal lobe and intermediate portion of left UF, the temporal lobe portion of right UF and the entire bilateral AF, likewise some regional segments in the frontier portion of right CGC, the anterior portion of left CGH and the frontal lobe portion of left UF.

For pointwise comparison of AD, CD patients demonstrated partial AD elevation in the following certain locations of the tracts: the anterior portion of bilateral ATR, the superior and inferior portion of bilateral CST, the thalamic portion of left CGH, the anterior portion of left IFOF, the anterior and posterior portion of right IFOF, the temporal lobe portion of bilateral UF and the parietal lobe portion of bilateral AF, likewise some regional segments in the frontal lobe portion of anterior CCF. Moreover, CD patients showed significant AD decrease in temporal lobe portion of bilateral CGH.

For pointwise comparison of RD, CD patients demonstrated widespread RD elevation in the following certain locations of the tracts: the anterior portion of bilateral ATR, the occipital lobe portion of posterior CCF, the frontal lobe portion of anterior CCF, the anterior and posterior portion of bilateral IFOF, the entire bilateral ILF and SLF, the temporal lobe and intermediate portion of left UF, the temporal lobe portion of right UF, the entire bilateral AF except for a temporal segment of left AF, likewise some regional segments in the intermediate portion of anterior CCF and the frontal lobe portion of left UF.

3.4. Correlation analysis

In the correlation analysis between clinical characteristics and average FA of significantly changed fiber tracts relative to HC individuals, we found positive correlations between MMSE score and left SLF, and between MoCA score and the following tracts: anterior CCF, bilateral ILF and left SLF; Negative correlations were found between ACTH of 8:00 and the following tracts: anterior CCF and left ILF, and between ACTH of 16:00 and left ILF (Fig. 3). For the average MD correlation analysis, negative correlations were found between MMSE score and the following tracts: bilateral CGC, ILF and AF, anterior CCF, right IFOF, right SLF, right UF, and between MoCA score and the following tracts: bilateral CGC, ILF, SLF and AF, right CST, anterior CCF, right IFOF, right UF. Positive correlations were found between ACTH of 8:00 and the following tracts: anterior CCF and right IFOF (Fig. 4).

For the further correlation analysis between clinical characteristics and FA or MD profiles of significantly altered locations along fiber tracts relative to HC individuals, we found an extensive positive correlation between FA profile of the fiber tracts and cognitive performance (MMSE and MoCA) and a negative correlation between specific locations on FA profile of the fiber tracts and psychological deficits (SAS) or endocrinologic features (ACTH and cortisol). Detailed results were organized in supplementary Tables 1 and 2, and only ≥3 consecutive nodes were reported.

4. Discussion

Much more consistency for white matter than gray matter with neuropsychological symptoms indicate the significance of white matter in the pathogenesis of hypercortisolism-induced neuropsychological deficits. Yet constrained by the present approaches, most of these studies have suffered from a lack of clarity in defining the microstructural pattern of white matter. Moreover, issues about whether these abnormalities are localized to specific positions or spread along the tract had made it a more complicated situation. Using a new algorithm, the present study, extracting diffusion properties (FA, MD, AD and RD) at 100 anatomically equivalent locations along 20 main tracts in the brain, mapped the microstructural pattern of white matter abnormality in a relatively large cohort of patients with Cushing's disease. In line with previous studies (Bauduin et al., 2018; Jiang et al., 2017a; Jiang et al., 2019; van der Werff et al., 2014), the Microstructural pattern of white matter in Cushing's disease showed a widespread MD, RD increase, FA decrease and partial AD increase among tracts, mainly in CCF, IFOF, ILF, SLF, UF, and AF. While within the same tract abnormalities localized to specific positions. Besides, although demographic features did not differ between the two groups, more severe neuropsychological deficits were exhibited in CD patients. The current study elucidated the effect of cortisol or ACTH excess on the microstructural pattern of white matter and associated emotional and cognitive deficits in Cushing's disease, which may shed light on the pathogenesis of hypercortisolism-induced neuropsychological disorders and help early identification and intervention of Cushing's disease.

Derived from the DTI technique, which can reconstruct white matter architecture, diffusion parameters depict microstructural white matter abnormalities by assessing the motion of water molecules across and along the fibers and is influenced by physical properties of the fiber tract, such as axon density, degree of myelination and water volume (Johansen-Berg and Rushworth, 2009). For instance, reduced FA indicates compromise of fiber coherence and therefore white matter integrity. Elevated MD among tracts may suggest demyelination, or edema in fiber tracts (Alexander et al., 2007; Budde et al., 2009). More specifically, AD measures diffusivity parallel to the tract and relates to axonal integrity (Budde et al., 2009). RD measures diffusivity perpendicular to the tract and relates to myelin integrity. Therefore, extensively reduced FA and elevated MD, RD and partially increased AD among tracts in the CD patients may indicate loss of axons, demyelination, or edema in fiber tracts (Alexander et al., 2007; Budde et al., 2009). Nevertheless, we should interpret the microstructural features of white matter inferred from tensor metrics with caution since they are indirect measures of the real biologic structure.

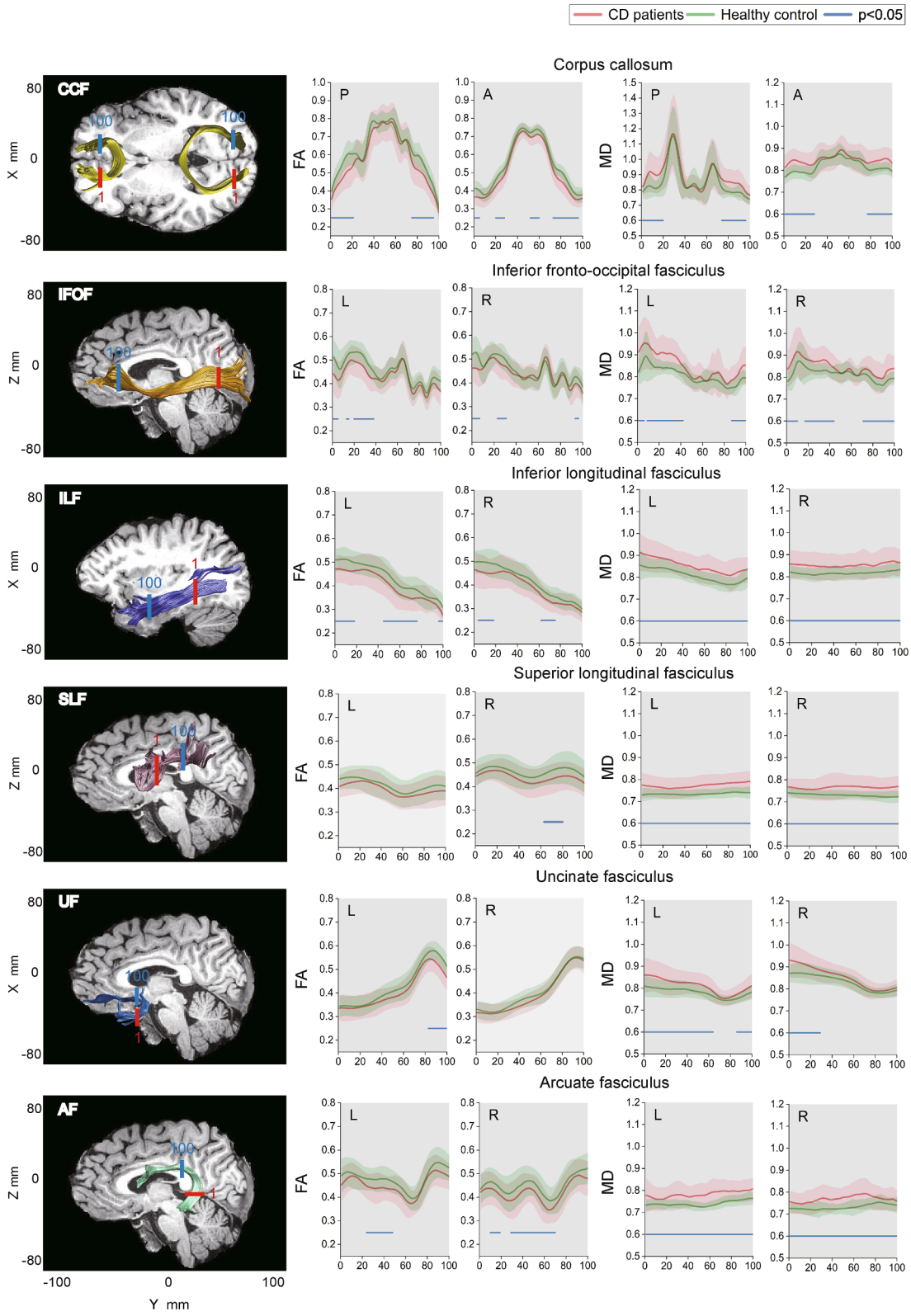

Fig. 1. The Pointwise Comparison of Fractional Anisotropy (FA) and Mean Diffusivity (MD) Profiles Between CD patient Group and Healthy Control Group.In the left, T1 structural images show renderings of 6 significantly altered tracts identified by Automated Fiber Quantification. The portions between waypoint ROIs (The red ROIs represent the starting ROIs and the blue ROIs represent the ending ROIs.) were the central part of the tract which were segmented and analyzed in this study. The plots of FA and MD profiles of 20 identified fiber tracts from Cushing's disease patients and healthy control individuals (red for Cushing's disease patients and green for healthy control individuals) are presented in mean (SD) (solid line for means and shaded areas for SDs). The blue bar under the FA and MD profile means the regions of significant difference between Cushing's disease patients and healthy control individuals. The Y-axis represents the FA or MD value. The X-axis represents the location between the beginning and termination waypoint regions of interest. Abbreviation: P indicates posterior; A, anterior; L, left; R, right. (For interpretation of the references to color in this figure legend, the reader is referred to the web version of this article.)

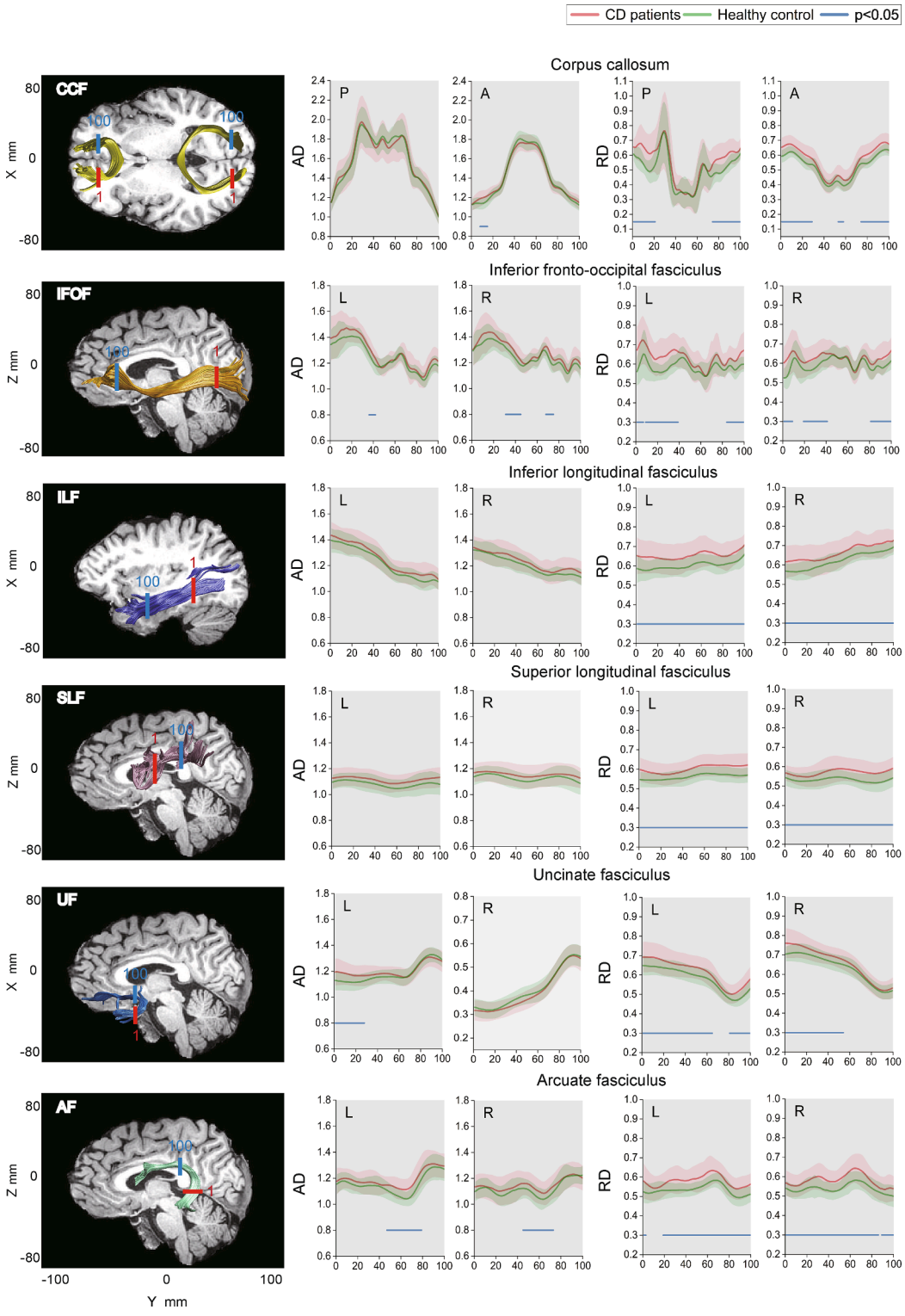

Fig. 2. The Pointwise Comparison of Axial Diffusivity (AD) and Radial Diffusivity (RD) Profiles Between CD patient Group and Healthy Control Group. In the left, T1 structural images show renderings of 6 significantly altered tracts identified by Automated Fiber Quantification. The portions between waypoint ROIs (The red ROIs represent the starting ROIs and the blue ROIs represent the ending ROIs.) were the central part of the tract which were segmented and analyzed in this study. The plots of AD and RD profiles of 20 identified fiber tracts from Cushing's disease patients and healthy control individuals (red for Cushing's disease patients and green for healthy control individuals) are presented in mean (SD) (solid line for means and shaded areas for SDs). The blue bar under the AD and RD profiles means the regions of significant difference between Cushing's disease patients and healthy control individuals. The Y-axis represents the AD or RD value. The X-axis represents the location between the beginning and termination waypoint regions of interest. Abbreviation: P indicates posterior; A, anterior; L, left; R, right. (For interpretation of the references to color in this figure legend, the reader is referred to the web version of this article.)

Such global alterations might be explained from and summarized in two aspects, the direct and indirect effects of cortisol on white matter. The integrity of changes in the white matter according to reduction in FA and elevation in MD, AD and RD is directly involved with neuron, oligodendrocyte (van der Werff et al., 2014). Hence, the direct effect of hypercortisolism on microstructural pattern might be interpreted in terms of neurons and oligodendrocytes. First, neurons act as the basis of white matter and their axons conducts neural signals among different gray matter regions (Lebel and Deoni, 2018). Gray matter atrophy and loss of neurons have been reported in many CD studies (Andela et al., 2013; Bauduin et al., 2018). Excess cortisol, associated with cell death, was known to reduce neurogenesis and neurotrophic factors (Bhatt et al., 2013; Sapolsky et al., 1986; Wang et al., 2011). Evidence from animal and cell studies indicates that hypercortisolism can modify the dendrite and spine morphology resulting in branch simplification and retraction (Kleen et al., 2006). Subsequent synapse loss would block the transmission of neurotrophic factors which would, in turn, aggravate the deficits in white matter integrity (Tata et al., 2006) leading to FA and AD

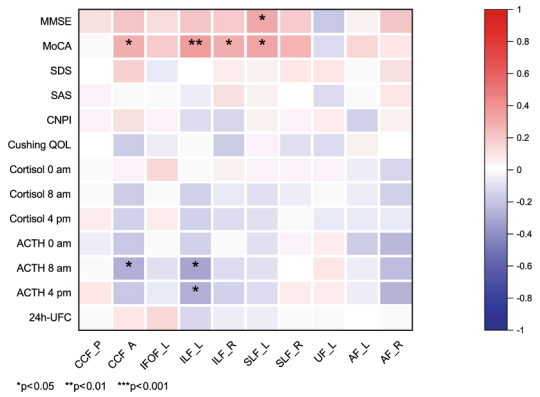

Fig. 3. Correlation analysis between clinical features and mean FA of significantly altered fiber tracts. Results of correlation analysis are presented as a correlation coefficient matrix. Red indicates positive correlation and blue indicate negative correlation. The shades of color indicate the degree of correlation. Abbreviation: MMSE, Mini-Mental State Examination; MoCA, Montreal Cognitive Assessment; SDS, Self-Rating Depression Scale; SAS, Self-Rating Anxiety Scale; CNPI, Chinese version of the neuropsychiatric inventory; Cushing QOL, Cushing's Quality of Life questionnaire; ACTH, adrenocorticotropic hormone; 24 h-UFC, 24 h-urinary free cortisol; CCF, corpus callosum forceps; IFOF, inferior fronto-occipital fasciculus; ILF, inferior longitudinal fasciculus; SLF, superior longitudinal fasciculus; UF, uncinated fasciculus. AF, arcuate fasciculus. L, left; R, right; P, posterior; A, anterior. (For interpretation of the references to color in this figure legend, the reader is referred to the web version of this article.)

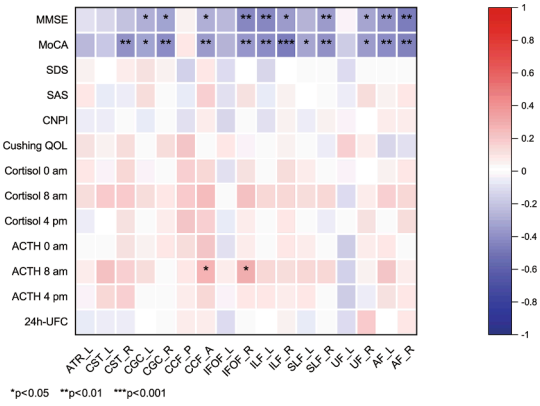

Fig. 4. Correlation analysis between clinical features and mean MD of significantly altered fiber tracts. Results of correlation analysis are presented as a correlation coefficient matrix. Red indicates positive correlation and blue indicate negative correlation. The shades of color indicate the degree of correlation. Abbreviation: MMSE, Mini-Mental State Examination; MoCA, Montreal Cognitive Assessment; SDS, Self-Rating Depression Scale; SAS, Self-Rating Anxiety Scale; CNPI, Chinese version of the neuropsychiatric inventory; Cushing QOL, Cushing's Quality of Life questionnaire; ACTH, adrenocorticotropic hormone; 24 h-UFC, 24 h-urinary free cortisol; ATR, anterior thalamic radiation; CST, corticospinal tract; CGC, cingulum cingulate; CGH, cingulum hippocampus; CCF, corpus callosum forceps; IFOF, inferior fronto-occipital fasciculus; ILF, inferior longitudinal fasciculus; SLF, superior longitudinal fasciculus; UF, uncinated fasciculus. AF, arcuate fasciculus. L, left; R, right; P, posterior; A, anterior. (For interpretation of the references to color in this figure legend, the reader is referred to the web version of this article.)

reduction. Intriguingly, among these significantly compromised tracts (FA decreased, MD and RD increased tracts), AD, which indicates axonal integrity, partially, increased instead. This may be result from increased edema caused by excess cortisol which would increase diffusivity in all directions. Second, oligodendrocytes account for the myelination of axons associated with nerve conduction velocity and thus with processing speed (Gutiérrez et al., 1995). Previous studies have reported that myelin lamellae fail to associate and compact after prolonged exposure to excess cortisol showing a more open and loose myelin conformation which indicates the reorganization of myelin (Chari, 2014). Of note, hypercortisolism also has been proved to inhibit the proliferation of oligodendrocyte precursors in animal models (Alonso, 2000; Miyata et al., 2011). In this manner, chronic exposure to elevated cortisol levels would lead to demyelination of axons, thus causing abnormal alterations in white matter integrity with FA reduced and RD, MD elevated.

Another explanation may be the indirect effect of cortisol. Classic view believed that cortisol is universally anti-inflammatory, however previous studies revealed that chronic exposure to hypercortisolism could be pro-inflammatory and impair the central nervous system. Cortisol exerts its versatile effects by activating specific receptors (mineralocorticoid receptor and glucocorticoid receptor), yet long-term exposure to high dose cortisol would form cortisol resistance which might be characterized by a decrease in glucocorticoid receptor function (Sorrells and Sapolsky, 2007). Thus, chronic exposure to hypercortisolism initiated neuroinflammation instead, including pro-inflammatory cell migration (Dinkel et al., 2004), cytokine production (Dhabhar, 2002), and even transcription factor activity in the brain (Bruccoleri et al., 1999). Neuroinflammation might increase extracellular water volume in the entire brain, then causing damage to white matter integrity (Syková and Nicholson, 2008). It was also noteworthy that increased cardiovascular risk factors, including hypertension, hyperglycemia, and dyslipidemia, caused by elevated concentration of cortisol in patients with Cushing's disease were also considered to be critical contributors to the white matter lesions (Santos et al., 2015; Williamson et al., 2018). Cardiovascular risk factors would result in loss of microvascular function with disordered cerebral hemodynamic, termed small vessel disease, and lead to ischemia and blood–brain barrier dysfunction which would further induce activated microglia, oligodendroglia apoptosis, clasmatodendritic astrocytosis and impair the white matter structure (Black et al., 2009; Moroni et al., 2020). Moreover, neurovascular decoupling following small vessel disease would fail to maintain the homeostasis of the cerebral microenvironment by compromising energy utilization and promoting aggregation of neurotoxic metabolites, such as amyloid-β peptide and tau protein (Iadecola, 2017), subsequently inducing chronic brain damage in vulnerable tracts associated with neuropsychological deficits. Notably, all these referred indirect factors could cause extracellular and intracellular edema resulting in diffusivity increase in all directions which may explain significant MD, AD, and RD increase among tracts. Furthermore, consistent with previous researches (Pires et al., 2015; Pires et al., 2017; van der Werff et al., 2014), significant MD, RD and AD increase with FA reduction rather than AD decrease with FA reduction may suggest underlying loss of white matter integrity predominantly caused by demyelination and edema. And these possibilities also raise the need to concern about the inflammatory and vascular state in the patients with chronic exposure to overdose cortisol for future study. Correspondingly potential targets for therapeutic intervention such as balance between pro- and anti-inflammation, cardiovascular risk reduction should be taken into consideration as well.

In line with previous studies (Jiang et al., 2017a; Pires et al., 2017; van der Werff et al., 2014), our finding revealed a widespread degeneration in white matter tract which may indicate the richness of cortisol receptors in the brain and versatility of cortisol. While the inconsistent results in comparison of diffusion metrics may indicate different severity and vulnerability among these tracts. As to the tracts (CCF, IFOF, ILF, SLF, UF, AF) altered significantly both in FA, RD and MD, deterioration may result from both myelin degradation, edema and axon loss exhibiting a more disrupted microstructural pattern. CCF, also known as splenium and genu of corpus callosum, are important commissural fibers connecting the homologous regions of the anterior frontal lobe and posterior occipital lobe (Paul et al., 2007). Converging evidence

suggested that CCF was associated with processing speed, executive function, visual object recognition and discrimination (Kerchner et al., 2012; Putnam et al., 2010). Besides, UF, a tract connecting orbitofrontal cortex and anterior cingulate cortex to amygdala, hippocampus and other limbic areas (Göttlich et al., 2014; Posner et al., 2014), alongside CCF was involved in frontal-limbic circuits. Disrupted frontal-limbic circuits may lead to emotive (anxiety and depression) and cognitive disorders (Berthier et al., 1996). Although relationship between cognitive deficits and posterior CCF was not identified in terms of mean FA or MD, correlations were detected by AFQ in profile of white matter fascicle highlighting its ability to identify structural abnormalities in detail. IFOF, involving attention processing, visual processing, emotion processing and cognitive function (Chanraud et al., 2010; Epstein et al., 2014), is a long cortio-cortical tract that connects the occipital lobe and frontal lobe with occipital gyrus, inferior middle occipital gyrus, whereas some researchers proposed that the IFOF also contain fibers connecting the frontal lobe to the posterior part of the temporal and parietal lobes (Fernández-Miranda et al., 2008). Given such controversy, posterm dissection and DTI suggested that tracts need to be segmented to more detailed subfractions catering to the thrust of AFQ which can offer us a more comprehensive understanding of anatomical features of WM and associated neuropsychological domains (Wu et al., 2016). SLF, linking the frontal, temporal, parietal and occipital lobes, were introduced to be responsible for emotional disorder and attention process (Klarborg et al., 2013; Lai and Wu, 2014). Together with CCF, IFOF and UF, SLF participates in or connect to the fronto-subcortical circuit which includes five different loops linking specific regions of the frontal lobe (motor cortex, supplementary motor cortex, dorsolateral prefrontal cortex, anterior cingulate cortex and orbitofrontal cortex) to thalamus, globus pallidus, substrantia nigra and striatum then return to the frontal lobe (Tekin and Cummings, 2002). Dysregulation of the fronto-subcortical circuit would cause memory loss and deficits in emotional and cognitive performance (Tekin and Cummings, 2002; Wang et al., 2012). Other than the fronto-subcortical circuit, SLF and UF also play critical roles in the medial temporal circuit with ILF (Maclean, 1952). The ILF connects the anterior temporal lobe to the extrastriate cortex of occipital lobe, extending along the inferior and lateral wall of the lateral ventricle. Diffusion tensor imaging studies revealed that damaged microstructure of ILF accounts for mood disorder and cognitive impairment such as dysregulated emotion processing, semantic disfluency, executive dysfunction and episodic memory loss (Chen et al., 2020; Sedda, 2014). The medial temporal circuit, also known as Papez's circuit, is integral for semantic cognition, episodic memory function, executive function and behavioral performance (Papez, 1995; Reijmer et al., 2013; Zhou et al., 2010). Therefore, in the present study, the observation of FA reduction and MD, RD elevation in CCF, IFOF, SLF, ILF, UF may support the hypothesis that disconnected microstructural pattern in fronto-subcortical circuit, frontal-limbic circuits and Papez's circuit plays a key role in the pathogenesis of mood disorder and cognitive deficit induced by chronic cortisol burden. With regard to cortex damage due to the high concentration of cortisol, several studies have reported prominent atrophy or functional disruption of frontal lobe, hippocampus, cingulate cortex and amygdala in patients with hypercortisolism as well (Bauduin et al., 2018; Crespo et al., 2014; Maheu et al., 2008). Since the involved cortices are important components of these circuits, our findings of disrupted microstructural pattern in white matter could be the result of secondary lesion due to the gray matter impairment. Intriguingly, in the current study, we also observed significantly damaged integrity of AF which is the tempro-frontal component of SLF and connects the primary auditory cortex to Wernicke's area and via Geschwind's area to Broca's area. AF is generally regarded to be involved in language processing and impairment of AF would lead to aphasia (Catani et al., 2005). However, in line with our findings, previous studies revealed that reduced integrity in AF may account for cognitive and intelligence decline (Ikuta et al., 2020; Kennedy and Raz, 2009; Lebel and Beaulieu, 2009). Of note, abnormalities distributed unevenly along white matter tract may indicate distinct vulnerability of different segments of the same fiber. It also gives us hint that different locations of the fiber may account for different cognitive or emotional domains, which may explain the diversity and complexity of neuropsychological symptoms among CD patients. Besides, tentative speculation was made on the potential mechanism that unevenly distribution may be a result of differences in developmental process and genetic variability among tracts and individuals (Chen et al., 2020; Sun et al., 2015). Despite these hypotheses, further studies are required to unmask the actual mechanism under the phenomenon.

To the best of our knowledge, our study might be the first to investigate and validate whole-brain white matter structure using automated fiber quantification and inspect each fiber tract and specific locations along the trajectory. Moreover, locations with microstructural impairment were conjugated with neuroendocrinological indices and neuropsychological deficits in CD patients, indicating a link of neuroendocrinological indices to neuropsychological performance through white matter microstructural pattern. Several limitations to this study need to be acknowledged. First, restricted by the tensor model, termed as the ellipsoid model which the fiber tractography based on, crossing-fiber in some voxels cannot be tracked properly. Furthermore, to avoid varied anatomy from superficial regions, only components between 2 waypoint ROIs before the tracts branch to the targeting gray matter were analyzed in this study. Probabilistic tractography based on ball & stick model and higher resolution techniques (High angular resolution diffusion MRI and Diffusion Spectrum Imaging) should be used to verify the results in future studies. Second, although we collected a relatively large cohort in this study despite the scarcity of CD cases, it may be insufficient to fully profile the microstructural pattern of white matter and uncover precise relations between white matter structure and clinical characteristics given the small absolute sample size. Thus, replication studies with a larger cohort are warranted to validate and refine the findings from the present study. Last but not the least, the observational nature of the current cross-sectional study excludes inferences about causality. A longitudinal study revealing dynamic alterations in white matter and their relationship with clinical features among CD patients in different stages of the disease (active, remitted and cured) is needed.

5. Conclusion

The current study emphasized the significance of white matter microstructural pattern in the pathogenesis of neuropsychological deficits in patients with hypercortisolism. In our cohort, CD patients showed widespread white matter pathology and specific lesion along the fiber with more severe cognitive decline. The findings suggest that the microstructural pattern of white matter may offer a promising biomarker for early identification and intervention of Cushing's disease.

Declaration of Competing Interest

The authors declare that they have no known competing financial interests or personal relationships that could have appeared to influence the work reported in this paper.

Acknowledgments

This study was supported by the National Natural Science Foundation of China (No. 82001798 and No. 81871087), Military Young Scholar Medical Research Fund of Chinese PLA General Hospital (No. QNF19071) and Medical Big Data and Artificial Intelligence Development Fund of Chinese PLA General Hospital (No.2019MBD-039).

Appendix A. Supplementary data

Supplementary data to this article can be found online at https://doi.

org/10.1016/j.nicl.2021.102770.

References

Alexander, A.L., Lee, J.E., Lazar, M., Field, A.S., 2007. Diffusion tensor imaging of the brain. Neurotherapeutics 4 (3), 316–329.

Alonso, G., 2000. Prolonged corticosterone treatment of adult rats inhibits the proliferation of oligodendrocyte progenitors present throughout white and gray matter regions of the brain. Glia 31 (3), 219–231.

Andela, C.D., van der Werff, S.J., Pannekoek, J.N., van den Berg, S.M., Meijer, O.C., van Buchem, M.A., Rombouts, S.A., van der Mast, R.C., Romijn, J.A., Tiemensma, J., Biermasz, N.R., van der Wee, N.J., Pereira, A.M., 2013. Smaller grey matter volumes in the anterior cingulate cortex and greater cerebellar volumes in patients with long-term remission of Cushing's disease: a case-control study. Eur. J. Endocrinol. 169, 811–819.

Basser, P.J., Pajevic, S., Pierpaoli, C., Duda, J., Aldroubi, A., 2000. In vivo fiber tractography using DT-MRI data. Magn. Reson. Med. 44 (4), 625–632.

Bauduin, S., van der Wee, N.J.A., van der Werff, S.J.A., 2018. Structural brain abnormalities in Cushing's syndrome. Curr. Opin. Endocrinol. Diabetes Obes. 25, 285–289.

Berthier, M.L., Kulisevsky, J., Gironell, A., Heras, J.A., 1996. Obsessive-compulsive disorder associated with brain lesions: clinical phenomenology, cognitive function, and anatomic correlates. Neurology 47 (2), 353–361.

Bhatt, A.J., Feng, Y., Wang, J., Famuyide, M., Hersey, K., 2013. Dexamethasone induces apoptosis of progenitor cells in the subventricular zone and dentate gyrus of developing rat brain. J. Neurosci. Res. 91 (9), 1191–1202.

Black, S., Gao, F., Bilbao, J., 2009. Understanding white matter disease: imaging-pathological correlations in vascular cognitive impairment. Stroke 40, S48–52.

Bruccoleri, A., Pennypacker, K.R., Harry, G.J., 1999. Effect of dexamethasone on elevated cytokine mRNA levels in chemical-induced hippocampal injury. J. Neurosci. Res. 57 (6), 916–926.

Budde, M.D., Xie, M., Cross, A.H., Song, S.-K., 2009. Axial diffusivity is the primary correlate of axonal injury in the experimental autoimmune encephalomyelitis spinal cord: a quantitative pixelwise analysis. J. Neurosci. 29 (9), 2805–2813.

Catani, M., Jones, D.K., ffytche, D.H., 2005. Perisylvian language networks of the human brain. Ann. Neurol. 57 (1), 8–16.

Chanraud, S., Zahr, N., Sullivan, E.V., Pfefferbaum, A., 2010. MR diffusion tensor imaging: a window into white matter integrity of the working brain. Neuropsychol. Rev. 20 (2), 209–225.

Chari, D.M., 2014. How do corticosteroids influence myelin genesis in the central nervous system? Neural Regen. Res. 9 (9), 909. https://doi.org/10.4103/1673-5374.133131.

Chen, H.-F., Huang, L.-L., Li, H.-Y., Qian, Y.i., Yang, D., Qing, Z., Luo, C.-M., Li, M.-C., Zhang, B., Xu, Y., 2020. Microstructural disruption of the right inferior fronto-occipital and inferior longitudinal fasciculus contributes to WMH-related cognitive impairment. CNS Neurosci. Ther. 26 (5), 576–588.

Crespo, I., Esther, G.-M., Santos, A., Valassi, E., Yolanda, V.-G., De Juan-Delago, M., Webb, S.M., Gómez-Ansón, B., Resmini, E., 2014. Impaired decision-making and selective cortical frontal thinning in Cushing's syndrome. Clin. Endocrinol. (Oxf) 81 (6), 826–833.

Dhabhar, F.S., 2002. Stress-induced augmentation of immune function–the role of stress hormones, leukocyte trafficking, and cytokines. Brain Behav. Immun. 16 (6), 785–798.

Dinkel, K., Dhabhar, F.S., Sapolsky, R.M., 2004. Neurotoxic effects of polymorphonuclear granulocytes on hippocampal primary cultures. Proc. Natl. Acad. Sci. U S A 101 (1), 331–336.

Epstein, K.A., Cullen, K.R., Mueller, B.A., Robinson, P., Lee, S., Kumra, S., 2014. White matter abnormalities and cognitive impairment in early-onset schizophrenia-spectrum disorders. J. Am. Acad. Child Adolesc. Psychiatry 53 (3), 362–372.e2.

Fernández-Miranda, J.C., Rhoton, A.L., Álvarez-Linera, J., Kakizawa, Y., Choi, C., de Oliveira, E.P., 2008. Three-dimensional microsurgical and tractographic anatomy of the white matter of the human brain. Neurosurgery 62 (Supp. 3), SHC989–SHC1028.

Forget, H., Lacroix, A., Somma, M., Cohen, H., 2000. Cognitive decline in patients with Cushing's syndrome. J. Int. Neuropsychol. Soc. 6 (1), 20–29.

Friston, K.J., 1998. The disconnection hypothesis. Schizophr. Res. 30 (2), 115–125.

Göttlich, M., Krämer, U.M., Kordon, A., Hohagen, F., Zurowski, B., 2014. Decreased limbic and increased fronto-parietal connectivity in unmedicated patients with obsessive-compulsive disorder. Hum. Brain Mapp. 35 (11), 5617–5632.

Gutiérrez, R., Boison, D., Heinemann, U., Stoffel, W., 1995. Decompaction of CNS myelin leads to a reduction of the conduction velocity of action potentials in optic nerve. Neurosci. Lett. 195 (2), 93–96.

Hattori, T., Yuasa, T., Aoki, S., Sato, R., Sawaura, H., Mori, T., Mizusawa, H., 2011. Altered microstructure in corticospinal tract in idiopathic normal pressure hydrocephalus: comparison with Alzheimer disease and Parkinson disease with dementia. AJNR Am. J. Neuroradiol. 32 (9), 1681–1687.

Hua, K., Zhang, J., Wakana, S., Jiang, H., Li, X., Reich, D.S., Calabresi, P.A., Pekar, J.J., van Zijl, P.C.M., Mori, S., 2008. Tract probability maps in stereotaxic spaces: analyses of white matter anatomy and tract-specific quantification. Neuroimage 39 (1), 336–347.

Iadecola, C., 2017. The neurovascular unit coming of age: a journey through neurovascular coupling in health and disease. Neuron 96 (1), 17–42.

Ikuta, T., Gollnick, H.M., Rutledge, A.N., 2020. Age associated decline in the arcuate fasciculus and IQ. Brain Imaging Behav. 14 (2), 362–367.

Jenkinson, M., Beckmann, C.F., Behrens, T.E., Woolrich, M.W., Smith, S.M., 2012. FSL. Neuroimage 62, 782–790.

Jenkinson, M., Smith, S., 2001. A global optimisation method for robust affine registration of brain images. Med. Image Anal. 5 (2), 143–156.

Jiang, H., He, N.-Y., Sun, Y.-H., Jian, F.-F., Bian, L.-G., Shen, J.-K., Yan, F.-H., Pan, S.-J., Sun, Q.-F., 2017a. Altered gray and white matter microstructure in Cushing's disease: A diffusional kurtosis imaging study. Brain Res 1665, 80–87.

Jiang, H., Liu, C., Pan, S.-J., Ren, J., He, N.-Y., Sun, Y.-H., Bian, L.-G., Yan, F.-H., Yang, W.-J., Sun, Q.-F., 2019. Reversible and the irreversible structural alterations on brain after resolution of hypercortisolism in Cushing's disease. Steroids 151, 108457. https://doi.org/10.1016/j.steroids.2019.108457.

Jiang, H., Ren, J., He, N.-Y., Liu, C., Sun, Y.-H., Jian, F.-F., Bian, L.-G., Shen, J.-K., Yan, F.-H., Pan, S.-J., Sun, Q.-F., 2017b. Volumetric magnetic resonance imaging analysis in patients with short-term remission of Cushing's disease. Clin. Endocrinol. (Oxf) 87 (4), 367–374.

Johansen-Berg, H., Rushworth, M.F.S., 2009. Using diffusion imaging to study human connectional anatomy. Annu. Rev. Neurosci. 32 (1), 75–94.

Kennedy, K.M., Raz, N., 2009. Aging white matter and cognition: differential effects of regional variations in diffusion properties on memory, executive functions, and speed. Neuropsychologia 47 (3), 916–927.

Kerchner, G.A., Racine, C.A., Hale, S., Wilheim, R., Laluz, V., Miller, B.L., Kramer, J.H., Stamatakis, E.A., 2012. Cognitive processing speed in older adults: relationship with white matter integrity. PLoS One 7 (11), e50425.

Klarborg, B., Skak Madsen, K., Vestergaard, M., Skimminge, A., Jernigan, T.L., Baaré, W. F.C., 2013. Sustained attention is associated with right superior longitudinal fasciculus and superior parietal white matter microstructure in children. Hum. Brain Mapp. 34 (12), 3216–3232.

Kleen, J.K., Sitomer, M.T., Killeen, P.R., Conrad, C.D., 2006. Chronic stress impairs spatial memory and motivation for reward without disrupting motor ability and motivation to explore. Behav. Neurosci. 120 (4), 842–851.

Lacroix, A., Feelders, R.A., Stratakis, C.A., Nieman, L.K., 2015. Cushing's syndrome. Lancet 386 (9996), 913–927.

Lai, C.-H., Wu, Y.-T., 2014. Alterations in white matter micro-integrity of the superior longitudinal fasciculus and anterior thalamic radiation of young adult patients with depression. Psychol. Med. 44 (13), 2825–2832.

Lebel, C., Beaulieu, C., 2009. Lateralization of the arcuate fasciculus from childhood to adulthood and its relation to cognitive abilities in children. Hum. Brain Mapp. 30 (11), 3563–3573.

Lebel, C., Deoni, S., 2018. The development of brain white matter microstructure. Neuroimage 182, 207–218.

León-Carrión, J., Atutxa, A.M., Mangas, M.A., Soto-Moreno, A., Pumar, A., Leon-Justel, A., Martín-Rodriguez, J.F., Venegas, E., Domínguez-Morales, M.R., Leal-Cerro, A., 2009. A clinical profile of memory impairment in humans due to endogenous glucocorticoid excess. Clin. Endocrinol. (Oxf) 70, 192–200.

MacLean, P.D., 1952. Some psychiatric implications of physiological studies on frontotemporal portion of limbic system (visceral brain). Electroencephalogr. Clin. Neurophysiol. 4 (4), 407–418.

Maheu, F.S., Mazzone, L., Merke, D.P., Keil, M.F., Stratakis, C.A., Pine, D.S., Ernst, M., 2008. Altered amygdala and hippocampus function in adolescents with hypercortisolemia: a functional magnetic resonance imaging study of Cushing syndrome. Dev Psychopathol 20 (4), 1177–1189.

Miyata, S., Koyama, Y., Takemoto, K., Yoshikawa, K., Ishikawa, T., Taniguchi, M., Inoue, K., Aoki, M., Hori, O., Katayama, T., Tohyama, M., Yoshikawa, T., 2011. Plasma corticosterone activates SGK1 and induces morphological changes in oligodendrocytes in corpus callosum. PLoS One 6 (5), e19859.

Momose, K.J., Kjellberg, R.N., Kliman, B., 1971. High incidence of cortical atrophy of the cerebral and cerebellar hemispheres in Cushing's disease. Radiology 99 (2), 341–348.

Moroni, F., Ammirati, E., Hainsworth, A.H., Camici, P.G., 2020. Association of white matter hyperintensities and cardiovascular disease: the importance of microcirculatory disease. Circ Cardiovasc Imaging 13 (8). https://doi.org/10.1161/CIRCIMAGING.120.010460.

Nieman, L.K., Biller, B.M.K., Findling, J.W., Murad, M.H., Newell-Price, J., Savage, M.O., Tabarin, A., 2015. Treatment of cushing's syndrome: an endocrine society clinical practice guideline. J. Clin. Endocrinol. Metab. 100 (8), 2807–2831.

Papez, J.W., 1995. A proposed mechanism of emotion. 1937. J. Neuropsychiatry Clin Neurosci 7, 103–112.

Paul, L.K., Brown, W.S., Adolphs, R., Tyszka, J.M., Richards, L.J., Mukherjee, P., Sherr, E. H., 2007. Agenesis of the corpus callosum: genetic, developmental and functional aspects of connectivity. Nat. Rev. Neurosci. 8 (4), 287–299.

Piasecka, M., Papakokkinou, E., Valassi, E., Santos, A., Webb, S.M., Vries, F., Pereira, A. M., Ragnarsson, O., 2020. Psychiatric and neurocognitive consequences of endogenous hypercortisolism. J. Intern. Med. 288 (2), 168–182.

Pires, P., Santos, A., Vives-Gilabert, Y., Webb, S.M., Sainz-Ruiz, A., Resmini, E., Crespo, I., de Juan-Delago, M., Gómez-Anson, B., 2015. White matter alterations in the brains of patients with active, remitted, and cured cushing syndrome: a DTI study. AJNR Am. J. Neuroradiol. 36 (6), 1043–1048.

Pires, P., Santos, A., Vives-Gilabert, Y., Webb, S.M., Sainz-Ruiz, A., Resmini, E., Crespo, I., de Juan-Delago, M., Gómez-Anson, B., 2017. White matter involvement on DTI-MRI in Cushing's syndrome relates to mood disturbances and processing speed: a case-control study. Pituitary 20 (3), 340–348.

Posner, J., Marsh, R., Maia, T.V., Peterson, B.S., Gruber, A., Simpson, H.B., 2014. Reduced functional connectivity within the limbic cortico-striato-thalamo-cortical loop in unmedicated adults with obsessive-compulsive disorder. Hum Brain Mapp. 35 (6), 2852–2860.

Putnam, M.C., Steven, M.S., Doron, K.W., Riggall, A.C., Gazzaniga, M.S., 2010. Cortical projection topography of the human splenium: hemispheric asymmetry and individual differences. J. Cogn. Neurosci. 22 (8), 1662–1669.

Reijmer, Y.D., Leemans, A., Caeyenberghs, K., Heringa, S.M., Koek, H.L., Biessels, G.J., 2013. Disruption of cerebral networks and cognitive impairment in Alzheimer disease. Neurology 80 (15), 1370–1377.
Santos, A., Granell, E., Gómez-Ansón, B., Crespo, I., Pires, P., Vives-Gilabert, Y., Valassi, E., Webb, S.M., Resmini, E., 2017. Depression and anxiety scores are associated with amygdala volume in cushing's syndrome: preliminary study. Biomed. Res. Int. 2017, 1–7.
Santos, A., Resmini, E., Gómez-Ansón, B., Crespo, I., Granell, E., Valassi, E., Pires, P., Vives-Gilabert, Y., Martínez-Momblán, M.A., de Juan, M., Mataró, M., Webb, S.M., 2015. Cardiovascular risk and white matter lesions after endocrine control of Cushing's syndrome. Eur. J. Endocrinol. 173, 765–775.
Sapolsky, R.M., Krey, L.C., McEwen, B.S., 1986. The neuroendocrinology of stress and aging: the glucocorticoid cascade hypothesis. Endocr. Rev. 7 (3), 284–301.
Sedda, A., 2014. Disorders of emotional processing in amyotrophic lateral sclerosis. Curr. Opin. Neurol. 27, 659–665.
Smith, S.M., 2002. Fast robust automated brain extraction. Hum Brain Mapp. 17 (3), 143–155.
Sonino, N., Fava, G.A., 2001. Psychiatric disorders associated with Cushing's syndrome. Epidemiology, pathophysiology and treatment. CNS Drugs 15 (5), 361–373.
Sorrells, S.F., Sapolsky, R.M., 2007. An inflammatory review of glucocorticoid actions in the CNS. Brain Behav. Immun. 21 (3), 259–272.
Starkman, M.N., Gebarski, S.S., Berent, S., Schteingart, D.E., 1992. Hippocampal formation volume, memory dysfunction, and cortisol levels in patients with Cushing's syndrome. Biol. Psychiatry 32 (9), 756–765.
Sun, H., Lui, S.u., Yao, L.i., Deng, W., Xiao, Y., Zhang, W., Huang, X., Hu, J., Bi, F., Li, T., Sweeney, J.A., Gong, Q., 2015. Two patterns of white matter abnormalities in medication-naive patients with first-episode schizophrenia revealed by diffusion tensor imaging and cluster analysis. JAMA Psychiatry 72 (7), 678–686.
Syková, E., Nicholson, C., 2008. Diffusion in brain extracellular space. Physiol. Rev. 88 (4), 1277–1340.
Tata, D.A., Marciano, V.A., Anderson, B.J., 2006. Synapse loss from chronically elevated glucocorticoids: relationship to neuropil volume and cell number in hippocampal area CA3. J. Comp. Neurol. 498 (3), 363–374.
Tekin, S., Cummings, J.L., 2002. Frontal-subcortical neuronal circuits and clinical neuropsychiatry: an update. J. Psychosom. Res. 53 (2), 647–654.
Trethowan, W.H., Cobb, S., 1952. Neuropsychiatric aspects of Cushing's syndrome. AMA Arch. Neurol. Psychiatry 67, 283–309.
van der Werff, S.J.A., Andela, C.D., Nienke Pannekoek, J., Meijer, O.C., van Buchem, M. A., Rombouts, S.A.R.B., van der Mast, R.C., Biermasz, N.R., Pereira, A.M., van der Wee, N.J.A., 2014. Widespread reductions of white matter integrity in patients with long-term remission of Cushing's disease. Neuroimage Clin. 4, 659–667.
van der Werff, S.J.A., Pannekoek, J.N., Andela, C.D., Meijer, O.C., van Buchem, M.A., Rombouts, S.A.R.B., van der Mast, R.C., Biermasz, N.R., Pereira, A.M., van der Wee, N.J.A., 2015. Resting-state functional connectivity in patients with long-term remission of cushing's disease. Neuropsychopharmacology 40 (8), 1888–1898.
Wakana, S., Caprihan, A., Panzenboeck, M.M., Fallon, J.H., Perry, M., Gollub, R.L., Hua, K., Zhang, J., Jiang, H., Dubey, P., Blitz, A., van Zijl, P., Mori, S., 2007. Reproducibility of quantitative tractography methods applied to cerebral white matter. Neuroimage 36 (3), 630–644.
Wang, C., Stebbins, G.T., Medina, D.A., Shah, R.C., Bammer, R., Moseley, M.E., deToledo-Morrell, L., 2012. Atrophy and dysfunction of parahippocampal white matter in mild Alzheimer's disease. Neurobiol. Aging 33 (1), 43–52.
Wang, J., Barak, L.S., Mook Jr., R.A., Chen, W., 2011. Glucocorticoid hedgehog agonists in neurogenesis. Vitam. Horm. 87, 207–215.
Wang, X., Zhou, T., Wang, P., Zhang, L.i., Feng, S., Meng, X., Yu, X., Zhang, Y., 2019. Dysregulation of resting-state functional connectivity in patients with Cushing's disease. Neuroradiology 61 (8), 911–920.
Williamson, W., Lewandowski, A.J., Forkert, N.D., Griffanti, L., Okell, T.W., Betts, J., Boardman, H., Siepmann, T., McKean, D., Huckstep, O., Francis, J.M., Neubauer, S., Phellan, R., Jenkinson, M., Doherty, A., Dawes, H., Frangou, E., Malamateniou, C., Foster, C., Leeson, P., 2018. Association of cardiovascular risk factors with MRI indices of cerebrovascular structure and function and white matter hyperintensities in young adults. Jama 320 (7), 665–673.
Wu, Y., Sun, D., Wang, Y., Wang, Y., 2016. Subcomponents and connectivity of the inferior fronto-occipital fasciculus revealed by diffusion spectrum imaging fiber tracking. Front Neuroanat 10, 88.
Yeatman, J.D., Dougherty, R.F., Myall, N.J., Wandell, B.A., Feldman, H.M., Beaulieu, C., 2012. Tract profiles of white matter properties: automating fiber-tract quantification. PLoS One 7 (11), e49790.
Zhang, W., Olivi, A., Hertig, S.J., van Zijl, P., Mori, S., 2008. Automated fiber tracking of human brain white matter using diffusion tensor imaging. Neuroimage 42 (2), 771–777.
Zhang, Y., Zhou, T., Feng, S., Wang, W., Liu, H., Wang, P., Sha, Z., Yu, X., 2021. The chronic effect of cortisol on orchestrating cerebral blood flow and brain functional connectivity: evidence from Cushing's disease. Metabolism 115, 154432. https://doi.org/10.1016/j.metabol.2020.154432.
Zhou, J., Greicius, M.D., Gennatas, E.D., Growdon, M.E., Jang, J.Y., Rabinovici, G.D., Kramer, J.H., Weiner, M., Miller, B.L., Seeley, W.W., 2010. Divergent network connectivity changes in behavioural variant frontotemporal dementia and Alzheimer's disease. Brain 133, 1352–1367.